Improvement of interface thermal resistance for surface-mounted UV-LEDs using graphene oxide silicone composite

Renli Liang†, *Jiangnan Dai* †* , *Lei Ye*†, *Linlin Xu*†, *Yang Peng*‡, *Shuai Wang*†,

Jingwen Chen†, *Hanling Long*†, *and Changqing Chen*†

†Wuhan National Laboratory for Optoelectronics, Huazhong University of Science and Technology, Luoyu Road 1037, Wuhan, 430074, China

‡School of Mechanical Science & Engineering, Huazhong University of Science and Technology, Luoyu Road 1037, Wuhan, 430074, China

KEYWORDS: interface thermal resistance, graphene oxide silicone composite, ultraviolet light-emitting diodes, junction temperature, long-term stability.

1. The calculation of the volume ratio of the air gaps in bracket-bonding layer

The height of air gap in bracket-bonding layer is depended on the thickness of bonding materials. In this investigation, the thickness of solder layer is about 150 μm. Based on the geometric dimensioning of air gap as showed, the volume ratio of the air gaps in bracket-bonding layer (3.2 mm×3.2 mm) is 12.5% for this UV-LED after calculation, and it may be larger in other LEDs, for example, the volume ratio of the air gaps in SETi DUV-LED (**Figure. S1f**) is over 30%, in DOWN DUV-LED (**Figure. S1g**) is about 45.2 %, as shown in Table A1. Because the height and depth are the same as for bonding-layer and air gaps, the volume ratio of air gaps depends on the total length of air gaps.

TABLE S1. CALCULATION OF VOLUME RATIO OF LIST PRODUCTS

LEDs/ UV-LEDs	The total length of bracket-bonding layer (mm)	The total length of air gaps (mm)	volume ratio
(a)	9	1	11%

(b)	2.7	0.7	25.9%
(c)	6.35	1.38	21.7%
(d)	3.2	0.5	15.6%
(e)	7.44	2.68	36.0%
(f)	3.2	1	31.25%
(g)	3.1	1.4	45.2%

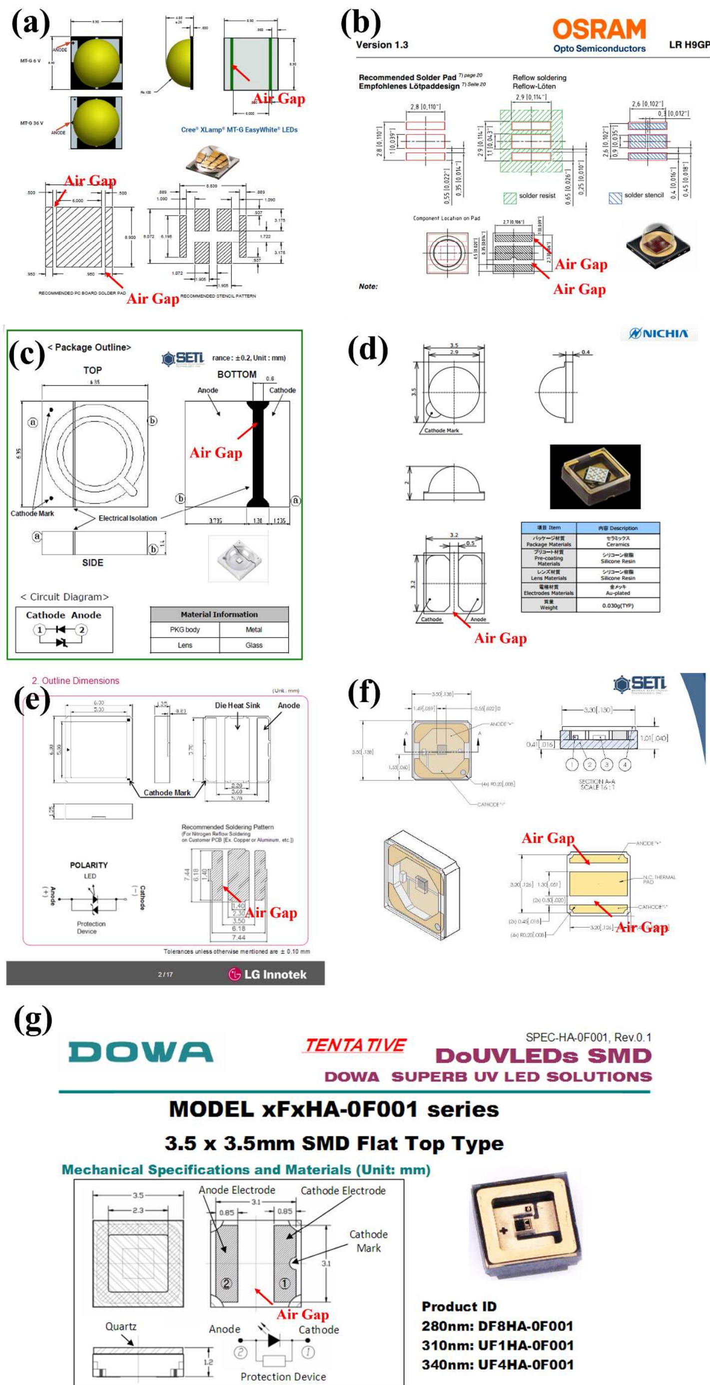

Figure S1. Products View of the surface mounted visible LED and UV-LED beads using ceramic bracket. (a) Cree XLamp MT-G Easywhite LEDs. (b) OSRAM LR H9GP. (c) SETi UV-LED. (d) NICHIA UV-LED, (e) LG DUV-LED. (f) SETi DUV-LED. (g) DOWA DUV-LED. Insulating layers must be designed and fabricated among the anode, cathode and thermal pad to form air gaps.

2. The simulation of proposed structure on thermal performance

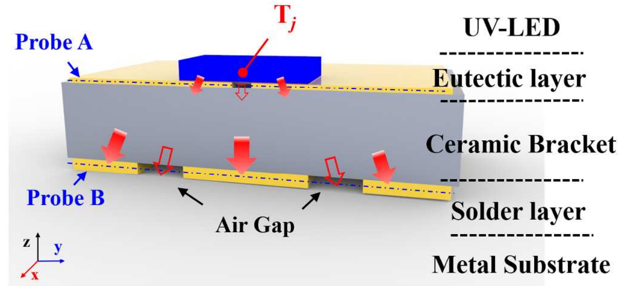

Figure S2. Thermal diffusion mode of the surface mounted UV-LED packaged on a metal substrate. Probe A and B represent the y-direction in center of die-bonding interface (eutectic layer) and bracket-bonding interface (solder layer), respectively.

TABLE S2. PROPERTIES OF MATERIAL AND STRUCTURE

MATERIAL	PROPERTIES		
	Thickness (μm)	**Thermal conductivity [W/(m·K)]**	**Thermal expansivity (/K)**
Eutectic layer	3	58	16×10^{-6}
Copper pad	80	383	18.5×10^{-6}
AlN ceramic bracket	635	170	4.5×10^{-6}
Copper pad& solder layer	150	53	21×10^{-6}
Metal substrate	1600	2	50×10^{-6}
Thermal interface material	100	1	/

Detailed three-dimensional device models with the reconstructed die-bonding thermal paths were established for FEA simulations. The temperature distribution of die-bonding interface and bracket-bonding interface was showed in **Figure S3** and **Figure S4**, respectively. The A represents the UV-LED without encapsulant embedded, but B, C, D, E, and F represent the UV-LEDs with thermal conductivity of 2, 4, 6, 8, 10 W/(m·K) encapsulants, respectively. It was observed that the decrease of

temperature distribution was improved as the thermal conductivity of encapsulant increased, which indicated that the heat dissipation was improved by providing the extra thermal paths. Meanwhile, the improvements in both die-bonding interface and bracket-bonding interface were weaken and reached saturation when the thermal conductivity of GO-based composite was beyond 6 W/(m·K).

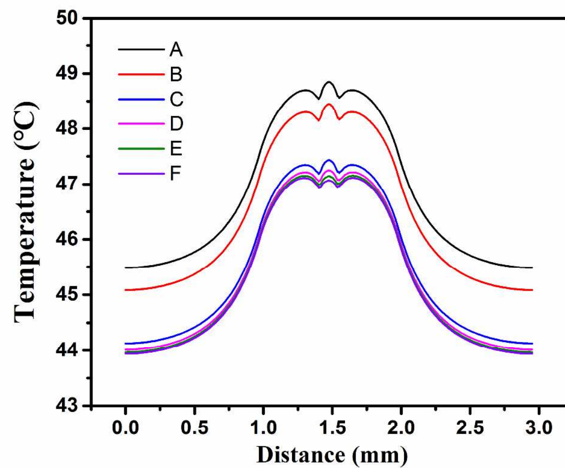

Figure S3. The temperature distribution of Probe A in eutectic layer.

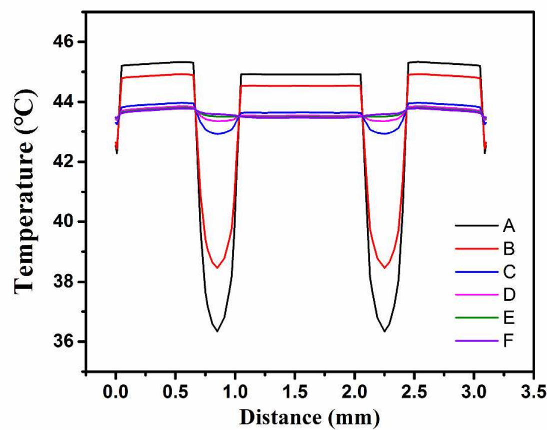

Figure S4. The temperature distribution of Probe B in solder layer.

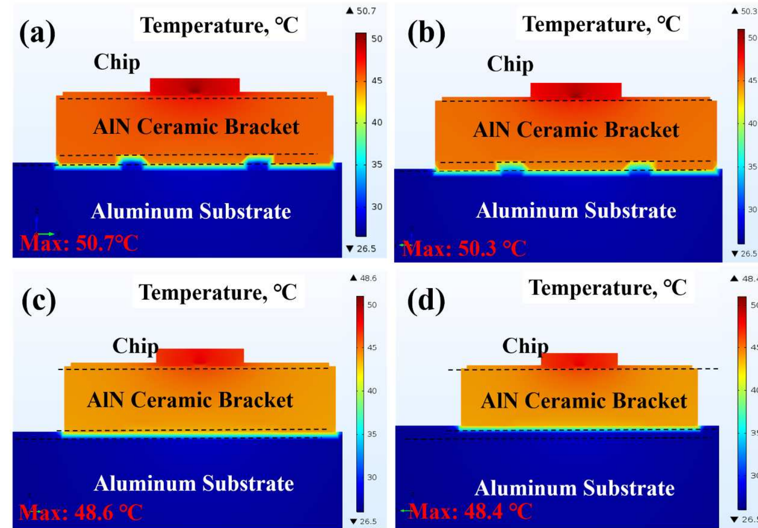

Figure S5. The cross section images of simulated temperature fields of UV-LED models. Traditional structure (a) without encapsulant; Proposed structure embedded by composite with thermal conductivity of (b) 2 W/(m·K); (c) 4 W/(m·K); (d) 6 W/(m·K).

The cross section images of simulated temperature fields of UV-LED models were shown in **Figure S5**. Much heat was gathered around air gaps and the highest temperatures located in the center of chip in traditional structure. But the proposed structure with encapsulant embedded possesses extra thermal paths to decrease the heat accumulation, leading to a decline of maximal temperature by 2.3 ℃ between the UV-LED without encapsulant embedded ant using encapsulant with thermal conductivity of 6 W/(m·k), as shown in Figure 5d. Based on the simulated results, the traditional and proposed structures using silicone composite with 4 wt% graphene oxide (GO) as filler were fabricated and investigated by measurement.

In addition, the mean temperatures of the active region top surface and aluminum

substrate bottom surface in the traditional structure are 48.49℃ and 25.96℃, respectively. But those in the proposed structure are 46.6℃ and 25.95℃. According to heat transfer theory, junction to substrate thermal resistance of UV-LED is defined as the temperature difference between the active region and heat sink divided by the heat flow. The following equation is established:

$$R_{th-js} = \frac{T_1 - T_2}{Q} \qquad (1)$$

where T_1 and T_2 are the mean temperatures of active region top surface and aluminum substrate bottom surface, and Q is the heat flow through. After calculation, the simulated $R_{th\text{-}js}$ of the traditional and proposed structures is 17.9 K/W and 16.6 K/W, respectively, showing a decrease of 1.3 K/W in total thermal resistance between the proposed structure and traditional structure, which is close to the measurement results shown in **Figure 6**. Furthermore, the average temperatures of active region were calculated at 48.5 ℃ and 46.9 ℃ for traditional structure and proposed structure, with a decrease of junction temperature by 1.6 ℃. The simulated results and experimental results both demonstrate the efficient reduction of interface thermal resistance and junction temperature of UV-LEDs by the proposed structure.

3. The measurement of light output power with traditional and proposed structure

The light output power of the UV-LEDs was measured using the ATA-1000 automatic photoelectric analysis system with a 30-cm-diameter integrating sphere, as shown in **Figure S6**. The light output power is enhanced after embedding the

GO-based composite. Benefited from the improvement of heat dissipation, the UV-LED with lower thermal resistance can express lower junction temperature, yielding a relatively higher light output power. Under the working current of 1000 mA, the light output powers are 950 mW and 992 mW for sample 1 and sample 1*, respectively, with an enhancement of 4.4% in the light output power, and the enhancement of 3.5% of light output power is found between sample 2 and sample 2*. Because the total thermal resistances of sample 2 and 2* are quite low, and the influence of junction temperature on LOP are decreased compared with sample 1 and sample 1*.

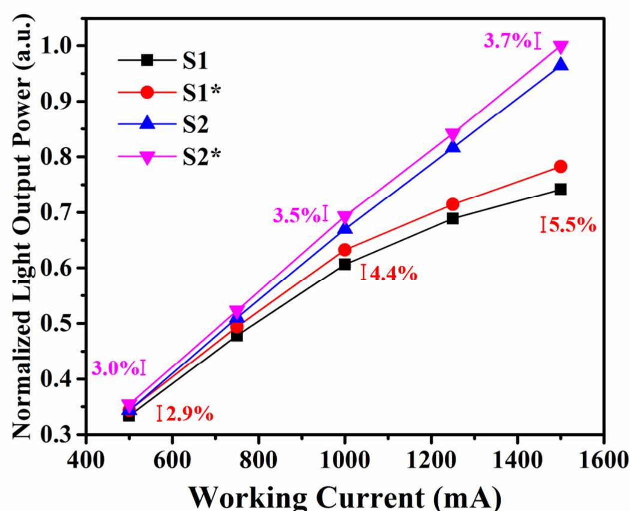

Figure S6. The normalized light output power comparison of samples before and after embedding GO-based composite.